

# Endocannabinoid signaling mediates oxytocin-driven social reward

Don Wei<sup>a</sup>, DaYeon Lee<sup>a</sup>, Conor D. Cox<sup>a</sup>, Carley A. Karsten<sup>a</sup>, Olga Peñagarikano<sup>b</sup>, Daniel H. Geschwind<sup>c,d</sup>, Christine M. Gall<sup>a</sup>, and Daniele Piomelli<sup>a,e,f,1</sup>

<sup>a</sup>Department of Anatomy and Neurobiology, University of California, Irvine, CA 92697; <sup>b</sup>Department of Pharmacology, School of Medicine, University of the Basque Country, Barrio Sarriena s/n, Leioa 48940, Spain; <sup>c</sup>Program in Neurogenetics, Department of Neurology, David Geffen School of Medicine, University of California, Los Angeles, CA 90095; <sup>d</sup>Center for Autism Research and Treatment and Center for Neurobehavioral Genetics, Jane and Terry Semel Institute for Neuroscience and Human Behavior, University of California, Los Angeles, CA 90095; <sup>e</sup>Department of Biological Chemistry, University of California, Irvine, CA 92697; and <sup>f</sup>Unit of Drug Discovery and Development, Istituto Italiano di Tecnologia, Genova 16163, Italy

Edited by Tomas G. M. Hokfelt, Karolinska Institutet, Stockholm, Sweden, and approved September 25, 2015 (received for review May 22, 2015)

**Marijuana exerts profound effects on human social behavior, but the neural substrates underlying such effects are unknown. Here we report that social contact increases, whereas isolation decreases, the mobilization of the endogenous marijuana-like neurotransmitter, anandamide, in the mouse nucleus accumbens (NAc), a brain structure that regulates motivated behavior. Pharmacological and genetic experiments show that anandamide mobilization and consequent activation of CB<sub>1</sub> cannabinoid receptors are necessary and sufficient to express the rewarding properties of social interactions, assessed using a socially conditioned place preference test. We further show that oxytocin, a neuropeptide that reinforces parental and social bonding, drives anandamide mobilization in the NAc. Pharmacological blockade of oxytocin receptors stops this response, whereas chemogenetic, site-selective activation of oxytocin neurons in the paraventricular nucleus of the hypothalamus stimulates it. Genetic or pharmacological interruption of anandamide degradation offsets the effects of oxytocin receptor blockade on both social place preference and cFos expression in the NAc. The results indicate that anandamide-mediated signaling at CB<sub>1</sub> receptors, driven by oxytocin, controls social reward. Deficits in this signaling mechanism may contribute to social impairment in autism spectrum disorders and might offer an avenue to treat these conditions.**

endocannabinoid | oxytocin | reward | social behavior | anandamide

Human studies have shown that marijuana heightens the saliency of social interactions (1), enhances interpersonal communication (2, 3), and decreases hostile feelings within small social groups (4). The neural mechanisms underlying these prosocial effects are unclear but are likely to involve activation of CB<sub>1</sub> cannabinoid receptors, the main molecular target of marijuana in the human brain (5). Consistent with this idea, CB<sub>1</sub> receptors are highly expressed in associational cortical regions of the frontal lobe and subcortical structures that underpin human social-emotional functioning (6, 7). Moreover, the receptors and their endogenous lipid-derived ligands, anandamide and 2-arachidonoyl-*sn*-glycerol (2-AG) (8), have been implicated in the control of social play (9) and social anxiety (10, 11), two crucial aspects of the social experience. Another essential facet of social behavior, the adaptive reinforcement of interactions among members of a group (i.e., the reward of being social), requires the oxytocin-dependent induction of long-term synaptic plasticity at excitatory synapses of the nucleus accumbens (NAc) (12), a key region in the brain reward circuit. Because the endocannabinoid system regulates the reinforcement of various natural stimuli (13) as well as NAc neurotransmission (14), in the present study we tested the hypothesis that this signaling complex might cooperate with oxytocin to control social reward.

## Results

**Anandamide Signaling at CB<sub>1</sub> Receptors Mediates Social Reward.** As a first test of the role of anandamide in social reward, we isolated juvenile, group-reared mice for 24 h and then either returned them to their group or left them in isolation for 3 additional hours (Fig.

1A). We then removed and snap-froze their brains, collected micro-punches from various regions of interest (Fig. S1), and measured endocannabinoid content by liquid chromatography-mass spectrometry. In contrast to conventional neurotransmitters, which are sequestered in storage vesicles and released by neurosecretion, the endocannabinoids are produced on-demand from membrane phospholipid precursors (15). For this reason, the tissue levels of these lipid substances provide an accurate estimate of mobilization (i.e., formation minus degradation) during signaling activity (8). We found that anandamide levels were substantially elevated in NAc and ventral hippocampus (vHC) of mice that had been returned to their group, compared with animals left in isolation (Fig. 1B). By contrast, no such changes were seen in the amygdala, dorsal striatum, ventral midbrain (comprising the ventral tegmental area and substantia nigra) (Fig. 1B) or other structures included in our survey (dorsal hippocampus, S2 cortex, and piriform cortex) (Fig. S2). Moreover, socialization did not change the levels of 2-AG (Fig. 1C and Fig. S3), an endocannabinoid substance (16–18) whose roles are often distinct from anandamide's (8); or the levels of oleoylethanolamide (Fig. 1D), a bioactive lipid that is structurally related to anandamide but acts through a distinct receptor mechanism (19). The results suggest that social contact stimulates anandamide mobilization in NAc and vHC, two regions of the mouse brain that are involved in the control of motivated behavior. Importantly, one of these regions, the NAc, has been recently implicated in the regulation of social reward by the hypothalamic neuropeptide oxytocin (12).

Interrupting the activity of fatty acid amide hydrolase (FAAH), the main anandamide-degrading enzyme in the brain, enhances the biological actions of this endocannabinoid neurotransmitter (20, 21). Therefore, to explore the function of socially driven anandamide mobilization, we tested juvenile mice lacking the *faah* gene in

## Significance

**We present evidence that an oxytocin-dependent endocannabinoid signal contributes to the regulation of social reward. The results provide insights into the functions of oxytocin, a neuropeptide crucial for social behavior, and its interactions with other modulatory systems that regulate the rewarding properties of social behavior. They further suggest that oxytocin-driven anandamide signaling may be defective in autism spectrum disorders, and that correcting such deficits might offer a strategy to treat these conditions.**

Author contributions: D.W. and D.P. designed research; D.W. and D.L. performed research; D.W., C.D.C., C.A.K., O.P., D.H.G., and C.M.G. contributed new reagents/analytic tools; D.W. and D.P. analyzed data; and D.W. and D.P. wrote the paper.

Conflict of interest statement: D.P. is an inventor on patents protecting a compound (URB597) used in the present study.

This article is a PNAS Direct Submission.

<sup>1</sup>To whom correspondence should be addressed. Email: piomelli@uci.edu.

This article contains supporting information online at [www.pnas.org/lookup/suppl/doi:10.1073/pnas.1509795112/-DCSupplemental](http://www.pnas.org/lookup/suppl/doi:10.1073/pnas.1509795112/-DCSupplemental).

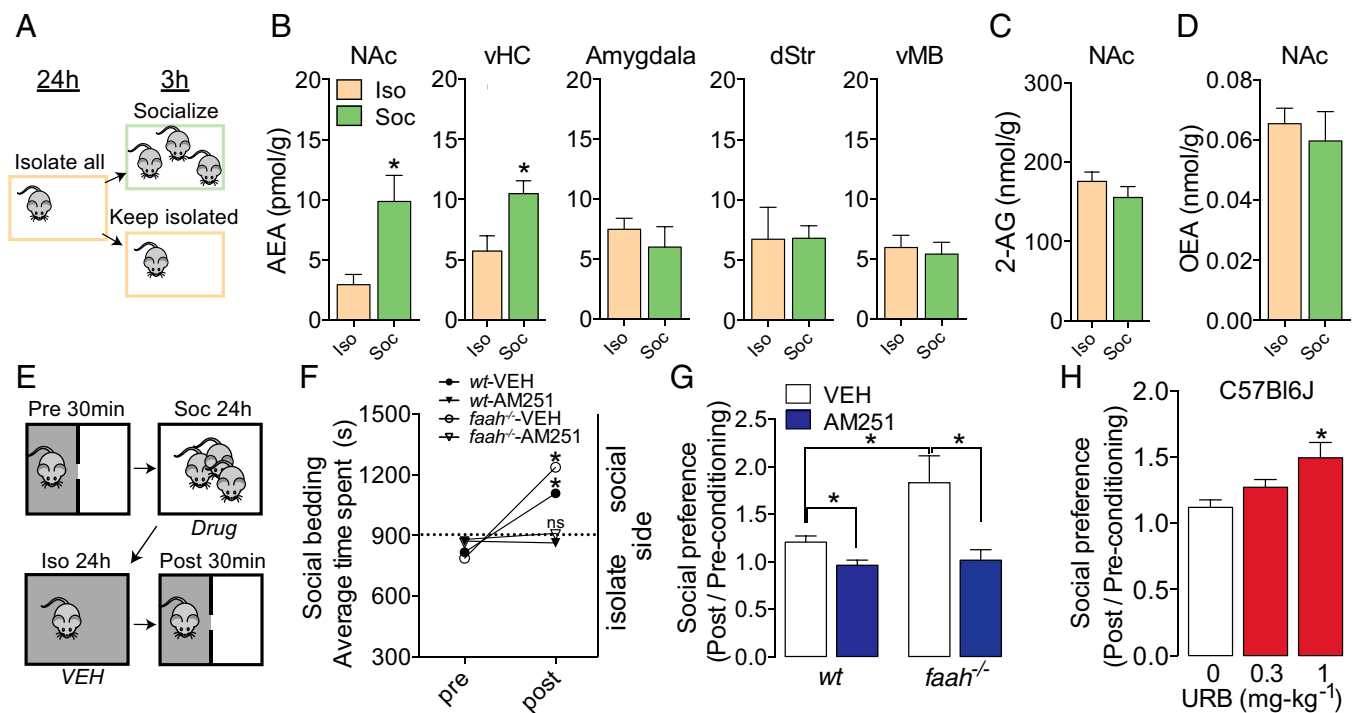


**Fig. 1.** Anandamide signaling at CB<sub>1</sub> receptors mediates social reward. (A) Schematics of the experimental protocol. (B–D) Levels of anandamide (AEA; B), 2-arachidonoyl-*sn*-glycerol (2-AG; C), and oleoylethanolamide (OEA; D) in nucleus accumbens (NAc), ventral-to-mid hippocampus (vHC), amygdala, dorsal striatum (dStr), and ventral midbrain (vMB) of isolated (Iso) or resocialized (Soc) C57Bl6 mice. (E) Schematics of the social conditioned place preference (sCPP) test. (F and G) sCPP in wild-type (wt) or *faah*<sup>-/-</sup> mice treated with vehicle (VEH) or CB<sub>1</sub> inverse agonist AM251 (2 mg·kg<sup>-1</sup>, intraperitoneal). (H) sCPP in mice treated with FAAH inhibitor URB597 (intraperitoneal). Data are shown as means ± SEM; \**P* < 0.05, compared using Student's unpaired *t* test, *n* = 4–5 (B–D), *n* = 12–14 (F), two-way ANOVA with Tukey's post hoc test, *n* = 12–14 (G), or one-way ANOVA with Bonferroni's post hoc test, *n* = 10 (H).

a conditioned place preference (CPP) task that specifically evaluates social reward (12) (Fig. 1E). Compared with their wild-type littermates, *faah*<sup>-/-</sup> mice displayed substantially higher levels of social CPP (sCPP) (Fig. 1F and G). This phenotypic difference was specific to social context, because CPP for high-fat food or cocaine was unchanged (Fig. S4), and was abolished by administration of the CB<sub>1</sub> antagonist AM251, which decreased place preference in both *faah*<sup>-/-</sup> and wild-type mice (Fig. 1F and G). Furthermore, the two genotypes showed similar performance levels in the three-chambered social approach task, which measures direct social approach behavior rather than social reward (Fig. S5).

Confirming FAAH's role and ruling out developmental compensation as a possible confounder, we noted that single systemic injections of the FAAH inhibitor URB597 (20) during the socialization phase of the test (Fig. 1E) replicated the prosocial phenotype seen in *faah*<sup>-/-</sup> mice in a dose-dependent manner (Fig. 1H). Furthermore, as seen with FAAH deletion, blocking FAAH with URB597 did not change performance in the social approach task (Fig. S5). Noteworthy, when the sCPP protocol was modified so that mice underwent isolation conditioning first, along with URB597 treatment, the subjects developed normal preference to the social context (Fig. S6), suggesting that enhancing anandamide signaling via FAAH inhibition increases social reward rather than decrease isolation aversion.

**Oxytocin Transmission Enhances Anandamide Mobilization in the Nucleus Accumbens.** A primary physiological function of oxytocin is to heighten the saliency of social stimuli (22). This effect may require the induction of long-term depression at excitatory synapses of the NAc, which receives direct oxytocinergic input from the paraventricular nucleus (PVN) of the hypothalamus (12). Therefore, we asked whether socialization-induced oxytocin neurotransmission might regulate anandamide signaling in the NAc, and obtained

three sets of results that supported this idea. First, systemic administration of the brain-permeant oxytocin receptor (OTR) antagonist, L-368,899, abolished the rises in anandamide levels elicited in NAc by social contact (Fig. 2A). Conversely, intracerebroventricular infusion of the OTR agonist WAY-267,464 elevated such levels in the absence of social contact and in an OTR-dependent manner (Fig. 2B). Lastly, and similarly to social stimulation, site-selective chemogenetic activation of oxytocin-secreting neurons in the PVN, which we previously showed to increase oxytocin transmission (23), increased anandamide mobilization in the NAc. Administration of clozapine-*N*-oxide (CNO) in mice engineered to express CNO receptors exclusively in oxytocinergic neurons of the PVN, strongly elevated anandamide content in the NAc, while having no effect on 2-AG (Fig. 2C and D). The same interventions produced a similar, but not identical, set of responses in the vHC. Intracerebroventricular administration of the OTR agonist WAY-267,464 increased anandamide levels (Fig. S7A), but oxytocinergic neuron activation with CNO produced only a trend toward increased anandamide mobilization, which was not statistically significant (Fig. S7B). Moreover, OTR blockade increased, rather than decreased, anandamide levels in the vHC (Fig. S7C). These results suggest that oxytocin transmission tightly controls anandamide mobilization in the NAc, but not the vHC, where its effects appear to be complex and possibly indirect.

**Anandamide Mediates Oxytocin-Dependent Social Reward.** If anandamide is a key mediator of the prosocial actions of oxytocin, as our findings seemingly imply, it follows that *faah*<sup>-/-</sup> mice, in which anandamide signaling is constitutively hyperactive, should be less sensitive than wild-type mice to the antisocial effects of OTR blockade (12). Confirming this prediction, we found that administration of the OTR antagonist L-368,899 reduced sCPP in wild-type, but not *faah*<sup>-/-</sup> mice (Fig. 3A and B). The pattern of NAc activation, assessed using cFos immunolabeling, also

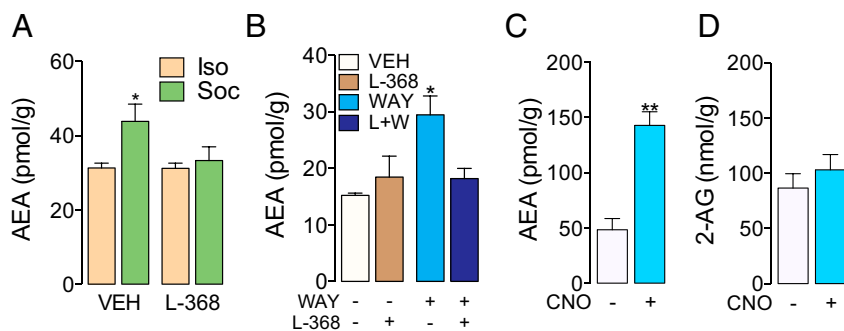


**Fig. 2.** Oxytocin transmission enhances anandamide mobilization in the nucleus accumbens (NAc). (A) Anandamide (AEA) levels in the NAc of isolated (Iso) or resocialized (Soc) mice treated with vehicle (VEH) or oxytocin receptor antagonist L-368,899 (5 mg·kg<sup>-1</sup>, intraperitoneal). (B) AEA levels in the NAc of isolated mice treated with the oxytocin agonist WAY-267,464 (5 nmol, intracerebroventricular), with or without the oxytocin receptor antagonist L-368,899 (0.5 nmol, intracerebroventricular). (C and D) Levels of AEA (C) and 2-AG (D) in the NAc of isolated mice with virally directed, oxytocin promoter-restricted expression of DREADD hM3Dq receptors in the paraventricular nucleus of the hypothalamus and were treated with VEH or clozapine-N-oxide (CNO, 5 mg·kg<sup>-1</sup>, intraperitoneal). Data are shown as means ± SEM; \**P* < 0.05, \*\**P* < 0.01, compared using two-way ANOVA with Tukey's post hoc test, *n* = 4–5 (A), one-way ANOVA with Bonferroni's post hoc test, *n* = 4–5 (B), or Student's unpaired *t* test, *n* = 4–5 (C and D).

provided indirect support to that hypothesis. Social contact (Fig. 1A) increased the number of cFos-positive cells in the NAc (Fig. 3C and D), and OTR blockade attenuated this effect only in wild-type mice (Fig. 3E and F), not in *faah*<sup>-/-</sup> mutants (Fig. 3G and H). The latter result cannot be attributed to reduced time spent socializing, because *faah*<sup>-/-</sup> mice displayed a similar amount of social interactions as did wild-type mice (Fig. S5). In contrast to the NAc, social contact did not significantly change the number of cFos-positive cells in the vHC, which was also unaltered by OTR blockade (Fig. S8).

## Discussion

The present study provides evidence that supports an obligatory role for anandamide in social reward. We show that (i) social contact stimulates anandamide mobilization in a brain region, the NAc, that is crucially involved in the reinforcing properties of natural stimuli (24), including social reward (12); (ii) this effect is prevented by blockade of the OTR and is mimicked by pharmacological or chemogenetic activation of this receptor; and (iii) heightened anandamide signaling (via FAAH inhibition) enhances social reward and occludes the prosocial effects of oxytocin. cFos expression experiments identify the shell region of the NAc as an important site in which this signaling mechanism might be operational.

In humans, marijuana can either facilitate or impair social interactions and social saliency, possibly depending on dose and context (1–3). Analogously, in animal models, cannabinoid receptor activation with direct-acting agonist drugs disrupts social interactions, whereas FAAH inhibition enhances them, which is suggestive of a role for anandamide in socialization (9, 25, 26). Although important, these data leave unanswered two key questions. The first is whether the anandamide, whose functions in the modulation of stress-coping responses are well recognized (10, 11, 20), might influence social behavior by modulating stress reactivity (27). We addressed this question with two complementary sets of experiments. In one, we used a model of socially conditioned place preference that focuses specifically on the acquisition of incentive salience (28). Mice were conditioned to social contact with familiar cage-mates for 24 h, an intervention that does not cause stress. When this conditioning procedure was paired with FAAH inhibition, or *faah*<sup>-/-</sup> mice were used instead of wild-type mice, the animals displayed a markedly increased preference for the social context. In separate studies, we evaluated the impact of genetic FAAH deletion or pharmacological FAAH blockade in the social approach task, in which mice are given the option of interacting with a novel conspecific or a novel object for a relatively short period (10 min). Socially normal mice spend more time with their conspecific than with the object. We found that neither

pharmacological nor genetic FAAH blockade had any effect in this model. Collectively, our findings support the conclusion that anandamide signaling at CB<sub>1</sub> receptors specifically regulates the incentive salience of social interactions, and that this effect is independent of anandamide's ability to modulate anxiety.

A second question addressed by the present work pertains to the neural circuits responsible for recruiting endocannabinoid neurotransmission during socialization. We used convergent experimental approaches to show that OTR activation by endogenously released oxytocin triggers anandamide mobilization in the NAc. This result is consistent with evidence indicating that oxytocin acts as a social reinforcement signal within this limbic region, where it elicits a presynaptic form of long-term depression (LTD) in medium spiny neurons (12). Thus, a plausible interpretation of our findings is that oxytocin triggers an anandamide-mediated paracrine signal in the NAc, which influences synaptic plasticity through activation of local CB<sub>1</sub> receptors. Activation of these receptors is known to induce presynaptic LTD at corticostriatal synapses (14, 29).

Although providing an economical explanation for our results, the hypothesis formulated above also raises several questions. Particularly important among them are questions about the roles that other modulatory neurotransmitters may play in regulating the interaction between oxytocin and anandamide. Previous studies point toward serotonin, which is needed for the expression of oxytocin-dependent plasticity in the NAc (12), and dopamine, which has been implicated in striatal anandamide signaling (30, 31). Defining such roles will require, however, further investigation.

In conclusion, our results illuminate a mechanism underlying the prosocial actions of oxytocin, and provide unexpected insights on possible neural substrates involved in the social facilitation caused by marijuana. Pharmacological modulation of oxytocin-driven anandamide signaling (by using, for example, FAAH inhibitors) might open new avenues to treat social impairment in autism spectrum disorders.

## Materials and Methods

**Animals.** We used juvenile male mice (4–8 wk) with C57Bl6J background. They were weaned at P21 and group-reared socially in cages of 4–5 animals each. Testing was done during the light cycle (on at 0630 h and off at 1830 h). All procedures met the National Institute of Health guidelines for the care and use of laboratory animals and were approved by the Institutional Animal Care and Use Committee at University of California, Irvine.

**Drug Preparation and Treatment.** We dissolved URB597 (synthesized in the laboratory) and AM251 (Cayman Chemicals) in a vehicle of saline/propylene glycol/Tween-80 (90/5/5, vol/vol). L-368,899 (Tocris) was dissolved in saline for

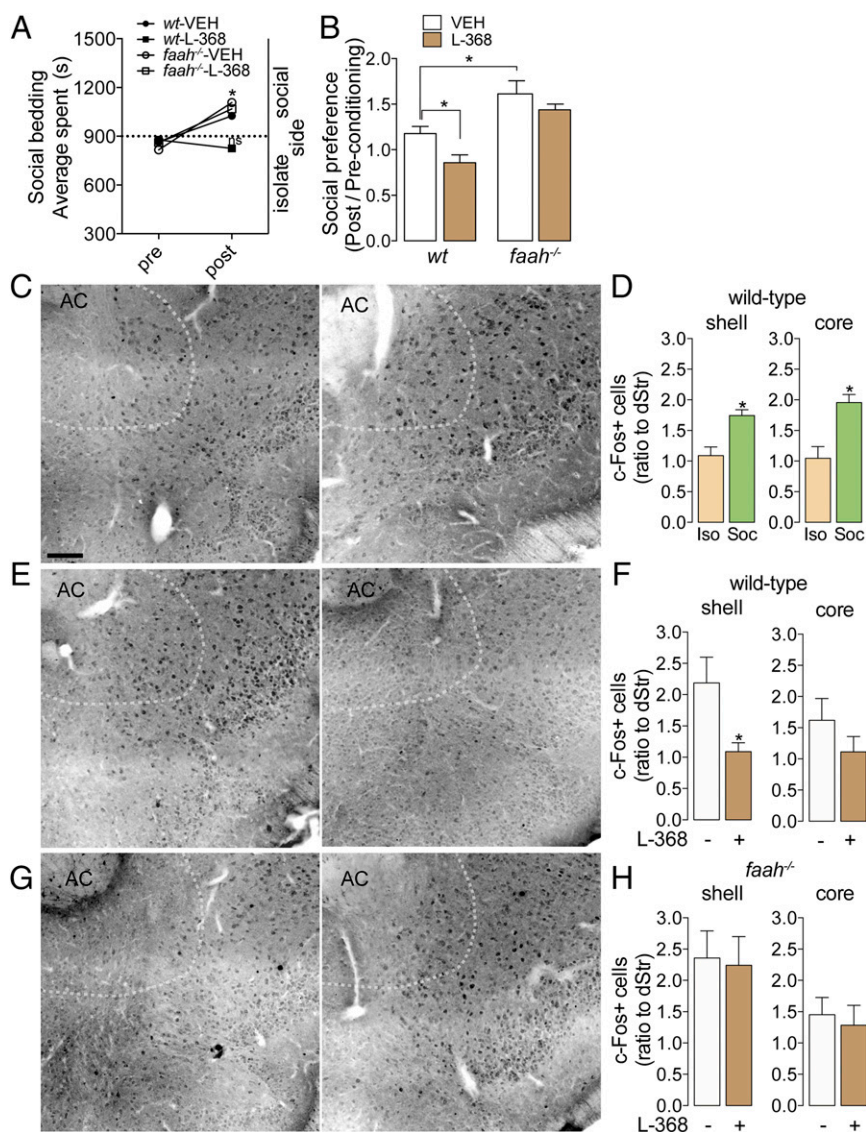


**Fig. 3.** Anandamide mediates oxytocin-dependent social reward. (A and B) sCPP of wild-type (wt) or *faah*<sup>-/-</sup> mice treated with vehicle (VEH) or oxytocin receptor antagonist L-368,899 (5 mg·kg<sup>-1</sup>, intraperitoneal). (C and D) Representative images and normalized quantification of cFos immunolabeling after isolation or resocialization, following the protocol in Fig. 1A. (E–H) cFos levels in socialized *faah*<sup>+/+</sup> mice and *faah*<sup>-/-</sup> mice treated with or without the oxytocin receptor antagonist L-368,899 (5 mg·kg<sup>-1</sup>, intraperitoneal). Scale bar represents 0.1 mm. Dotted line delineates core (inside) and shell (outside). Data are shown as means ± SEM; \**P* < 0.05, compared using Student's unpaired *t* test, *n* = 10–14 (A), *n* = 3–4 (C and D), *n* = 4–5 (E–H), or two-way ANOVA with Tukey's post hoc test, *n* = 10–14 (B).

i.p. injections or in DMSO for intracerebroventricular (i.c.v.) injections. WAY-267,464 (Tocris) was dissolved in DMSO. Clozapine-*N*-oxide (CNO, Tocris) and cocaine (Sigma-Aldrich) were dissolved in saline. For lipid analyses, L-368,899 was administered 0.5 h before the start of socialization (3.5 h before sacrifice), WAY-267,464 was administered by i.c.v. injection to 24-h isolated animals 0.5 h before sacrifice, and CNO to 24-h isolated animals 1 h before sacrifice. For the socially conditioned place preference (sCPP) test, animals were habituated to injections for 3 d leading up to the experiment. URB597, L-368,899 and AM251 were administered twice a day during social conditioning (AM/PM, i.p.). Balancing vehicle treatments were given during isolation conditioning (AM/PM). For the social approach task, URB597 was administered i.p. 3 h before starting the test.

**Intracerebroventricular (i.c.v.) Drug Infusions.** We anesthetized mice with ketamine-xylazine and stereotactically implanted a 22-gauge guide cannula (3.1 mm in length, Plastics One) positioned 1 mm above the right lateral ventricle at coordinates from bregma: AP -0.2, ML -1.0, and DV -1.3 mm (32). Animals were allowed to recover 10 d after surgery, during which they were maintained in social housing (groups of 2–3). Infusions were made in wake animals through a 33-gauge infusion cannula (Plastics One) that extended 1 mm beyond the end of the guide cannula. The injector was

connected to a 10- $\mu$ L Hamilton syringe by PE-20 polyethylene tubing. The syringe was driven by an automated pump (Harvard Apparatus) at a rate of 0.66  $\mu$ L/min to provide a total infusion volume of 0.5  $\mu$ L. Cannula placements were verified histologically.

**Recombinant Adeno-Associated (AAV) DREADD Virus.** We used a serotype 2 AAV vector that was previously constructed and validated to express a modified muscarinic receptor (hM3Dq) and the fluorescent protein mCherry (University of Pennsylvania Viral Core) (33). The hM3Dq receptor is exclusively activated by the otherwise inert compound clozapine-*N*-oxide. Expression of the virus is restricted by the oxytocin promoter, which directs oxytocin cell-specific expression of hM3Dq receptors and mCherry. mCherry expression in the paraventricular nucleus (PVN) was verified using a Leica 6000B epifluorescence microscope.

**Viral Infusions.** We bilaterally injected the AAV2-oxhM3Dq-mCherry construct into the PVN using the following coordinates (23): AP -0.70, ML  $\pm$ 0.30, and DV -5.20 mm. We used an adaptor with 33-G needle (Hamilton) connected via polyethylene tubing to a 10- $\mu$ L Hamilton syringe driven by an automated pump (Harvard Apparatus). We waited for 5 min before infusion in order for tissue to seal around the needle, infused a total volume of 0.5  $\mu$ L

( $\sim 10^{10}$  titer genome per mL) over 5 min and waited 10 min after infusion before removing the needle. Experiments were conducted 3 wk after viral injections to allow for recovery and adequate expression. During this period, animals were maintained in social housing (groups of 2–3).

**Brain Micropunches.** Whole brains were collected and flash-frozen in isopentane at  $-50$  to  $-60$  °C. Frozen brains were maintained in liquid nitrogen on the day of sacrifice until they were transferred to storage at  $-80$  °C. To take micropunches of brain tissue, we first transferred frozen brains to  $-20$  °C in a cryostat and waited 1 h for brains to attain local temperature. We then cut to the desired coronal depth and collected micropunches from bilateral regions of interest using a  $1 \times 1.5$ -mm puncher (Kopf Instruments). The micropunches weighed  $\sim 1.75$  mg. A reference micropunch was taken to normalize each punch to the brain's weight. Bilateral punches were combined for lipid analyses.

**Lipid Analyses.** Procedures were described (33). Briefly, tissue samples were homogenized in methanol containing internal standards for  $H^2$ -anandamide ( $H^2$ -AEA),  $H^2$ -oleoylethanolamide ( $H^2$ -OEA) and  $^2H_8$ -2-arachidonoyl-*sn*-glycerol ( $^2H_8$ -2-AG) (Cayman Chemicals). Lipids were separated by a modified Folch-Pi method using chloroform/methanol/water (2:1:1) and open-bed silica column chromatography. For LC/MS analyses, we used a 1100 liquid chromatography system coupled to a 1946D-mass spectrometer detector equipped with an electrospray ionization (ESI) interface (Agilent Technologies). The column was a ZORBAX Eclipse XDB-C18 ( $2.1 \times 100$  mm,  $1.8 \mu\text{m}$ , Agilent Technologies). We used a gradient elution method as follows: solvent A consisted of water with 0.1% formic acid, and Solvent B consisted of acetonitrile with 0.1% formic acid. The separation method used a flow rate of 0.3 mL/min. The gradient was 65% B for 15 min, then increased to 100% B in 1 min and kept at 100% B for 14 min. The column temperature was 15 °C. Under these conditions,  $Na^+$  adducts of anandamide/ $H^2$ -anandamide had retention times (Rt) of 6.9/6.8 min and *m/z* of 348/352, OEA/ $H^2$ -OEA had Rt 12.7/12.6 min and *m/z* 326/330, and 2-AG/ $^2H_8$ -2-AG had Rt 12.4/12.0 min and *m/z* 401/409. An isotope-dilution method was used for quantification (34).

**Perfusion and Immunohistochemistry.** Ketamine-xylazine anesthetized mice were perfused through the heart left ventricle, first with ice-cold saline solution and then with a fixation solution containing 4% (wt/vol) paraformaldehyde (PFA) in 0.1 M PBS (pH 7.4). Brains were collected, postfixed for 1.5 h and cryoprotected using 30% (wt/vol) sucrose in PBS. Coronal sections were cut using a microtome ( $30 \mu\text{m}$  thickness) and mounted on Superfrost plus slides (Fisher). For cFos immunostaining, sections were washed in 0.1 M glycine solution (in 0.1 M PBS) to quench excess PFA. Sections were incubated for 1 h in blocking solution (10% normal swine serum plus 0.3% Triton-X in 0.1 M PBS). Washed sections were incubated for 48 h at 4 °C with anti-cFos antibody (1:500, ab7963 from Abcam). After washing with 0.1 M PBS to remove unbound primary antibody, sections were then incubated for 1 h at room temperature with donkey anti-rabbit IgG conjugated to Alexa Fluor 594. Slides were coverslipped with Vectashield plus DAPI (Vector Labs). Images were captured using a 10x objective (Plan Apo, NA 0.4) on a Leica 6000B epifluorescence microscope with PCO Scientific CMOS camera and Metamorph acquisition software.

**cFos Quantification.** Image montages were stitched together using FIJI (35). Variability in background fluorescence was standardized by subtracting a Gaussian-blurred image of each image from itself. Objects of cellular size and shape were then detected using Python 2.7 and FIJI. Brain regions were traced by hand in FIJI using an atlas reference (32), and resulting coordinates were used to restrict cell counts. Because immunostaining varies across animals and experiments, values were normalized as a ratio to the dorsal striatum (dStr) of the same animal. The dStr was selected as an internal control because it did not vary across compared groups (Student's *t* test,  $n = 4$ –5).

**Socially Conditioned Place Preference (sCPP).** Following described procedures (12), mice were placed in an opaque acrylic box ( $27.3 \times 27.3$  cm), divided into two chambers by a clear acrylic wall with a small opening. In the box, a 30-min preconditioning test was used to establish baseline nonpreference to two types of autoclaved, novel bedding (Alpha Dry, PharmaServ; and Kaytee Soft Granules, Petco), which differed in texture and shade (white vs. dark

brown). Individual mice with strong preference for either type of bedding were excluded; typically, those that spent more than  $1.5\times$  time on one bedding over the other. The next day, animals were assigned to a social cage with cage-mates to be conditioned to one type of novel bedding for 24 h, then moved to an isolated cage with the other type of bedding for 24 h. Bedding assignments were counterbalanced for an unbiased design. Animals were then tested alone for 30 min in the two-chambered box to determine post-conditioning preference for either type of bedding. Fresh bedding was used at each step and chambers were thoroughly cleaned between trials with SCOE 10x odor eliminator (BioFOG, Alpharetta, GA) to avoid olfactory confounders. Volumes of bedding were measured to be consistent: 300 mL in each side of the two-chambered box and 550 mL in the home-cage. Animals from the same cage (and thus with familiar odors) were run concurrently in four adjacent, opaque CPP boxes. Scoring of chamber time and locomotion were automated using a validated image analysis script in ImageJ: The static background image was subtracted, moving objects of mouse shape and size were thresholded out and frames were counted in a position-restricted manner.

**Three-Chambered Social Approach Task.** Test mice were habituated to an empty three-chambered acrylic box ( $40.6 \times 21.6$  cm), as described (36). Habituation consisted of a 10-min trial in the center chamber with doors closed, and then a 10-min trial in all chambers with doors open. Then, during the 10-min testing phase, subjects were offered a choice between a novel object and a novel mouse in opposing side-chambers. The novel object was an empty inverted pencil cup and the novel social stimulus mouse was a sex-, age-, and weight-matched 129/SvImJ mouse. These mice were used because they are relatively inert, and they were trained to prevent aggressive or abnormal behaviors. Weighted cups were placed on top of the pencil cups to prevent climbing. Low lighting was used: All chambers were measured to be 5 lx. The apparatus was thoroughly cleaned with SCOE 10x odor eliminator (BioFOG) between trials to preclude olfactory confounders. Object/mouse side placement was counterbalanced between trials. Chamber time scoring was automated as in social CPP. Sniffing time was scored by trained assistants who were unaware of treatment conditions. Subjects with outlying inactivity or side preference were excluded.

**Cocaine and High-Fat Diet CPP.** These paradigms were largely similar to social CPP, including unbiased and counterbalanced design, cleaning and habituation, exclusion criteria, and scoring, except for the following key differences, which followed established methods (12, 37). Mice were conditioned and tested in a two-chambered opaque acrylic box ( $31.5 \times 15$  cm) with a small opening. Pre- and postconditioning tests allowed free access to both chambers and each had durations of 15 min (cocaine) and 20 min (high-fat). For conditioning, animals underwent 30-min sessions alternating each day between saline/cocaine (8 sessions total, 4 each) or standard chow pellet/high-fat pellet (12 sessions total, 6 each). The two chambers offered conditioning environments that differed in floor texture and wall pattern: sparse metal bars on the floor and solid black walls vs. dense-wire-mesh floors and striped walls. Sparse metal bars allowed for paw access to the smooth acrylic floor, whereas dense-wire mesh did not. For high-fat diet CPP, animals were given one pellet of standard chow and an isocaloric amount of high-fat food (Research Diets). As high-fat pellets have a different color and consistency, they were also given to home cages the day before preconditioning to prevent neophobia.

**Statistical Analyses.** Results are expressed as means  $\pm$  SEM. Significance was determined using two-tailed Student's *t* test, one-way or two-way analysis of variance (ANOVA) with Tukey's post hoc test and differences were considered significant if  $P < 0.05$ . Analyses were conducted using GraphPad Prism (GraphPad Software).

**ACKNOWLEDGMENTS.** We thank Dr. Dandan Li, Drake Dinh, Allison Anguren, Conor Murray, Kavi Peshawaria, Ernesto Paz, and Jennifer Lockney for help with experiments; Drs. Kwang-Mook Jung, Vidya Narayanaswami, Guillermo Moreno-Sanz, Julie Lauterborn, and Gul Dolen for valuable advice; and Terri Wang for her generous gift. This work was supported by the Autism Science Foundation Predoctoral Fellowship (to D.W.), National Institute of Health Grant DA012413 (to D.P.), the UC Irvine Medical Scientist Training Program, and the UC Irvine Center for Autism Research and Translation.

1. Tart CT (1970) Marijuana intoxication common experiences. *Nature* 226(5247):701–704.
2. Salzman C, Kochansky GE, Van Der Kolk BA, Shader RI (1977) The effect of marijuana on small group process. *Am J Drug Alcohol Abuse* 4(2):251–255.
3. Iversen LL (2001) *The Science of Marijuana* (Oxford Univ Press, Oxford).
4. Salzman C, Van Der Kolk BA, Shader RI (1976) Marijuana and hostility in a small-group setting. *Am J Psychiatry* 133(9):1029–1033.

5. Huestis MA, et al. (2007) Single and multiple doses of rimonabant antagonize acute effects of smoked cannabis in male cannabis users. *Psychopharmacology (Berl)* 194(4):505–515.
6. Glass M, Dragunow M, Faull RL (1997) Cannabinoid receptors in the human brain: A detailed anatomical and quantitative autoradiographic study in the fetal, neonatal and adult human brain. *Neuroscience* 77(2):299–318.
7. Seeley WW, Zhou J, Kim E-J (2012) Frontotemporal dementia: What can the behavioral variant teach us about human brain organization? *Neuroscientist* 18(4):373–385.

8. Piomelli D (2014) More surprises lying ahead. The endocannabinoids keep us guessing. *Neuropharmacology* 76(Pt B):228–234.
9. Trezza V, et al. (2012) Endocannabinoids in amygdala and nucleus accumbens mediate social play reward in adolescent rats. *J Neurosci* 32(43):14899–14908.
10. Bergamaschi MM, et al. (2014) Rimonabant effects on anxiety induced by simulated public speaking in healthy humans: A preliminary report. *Hum Psychopharmacol* 29(1):94–99.
11. Gunduz-Cinar O, et al. (2013) Convergent translational evidence of a role for anandamide in amygdala-mediated fear extinction, threat processing and stress-reactivity. *Mol Psychiatry* 18(7):813–823.
12. Dölen G, Darvishzadeh A, Huang KW, Malenka RC (2013) Social reward requires coordinated activity of nucleus accumbens oxytocin and serotonin. *Nature* 501(7466):179–184.
13. Fattore L, Melis M, Fadda P, Pistis M, Fratta W (2010) The endocannabinoid system and nondrug rewarding behaviours. *Exp Neurol* 224(1):23–36.
14. Robbe D, Kopf M, Remaury A, Bockaert J, Manzoni OJ (2002) Endogenous cannabinoids mediate long-term synaptic depression in the nucleus accumbens. *Proc Natl Acad Sci USA* 99(12):8384–8388.
15. Piomelli D, Astarita G, Rapaka R (2007) A neuroscientist's guide to lipidomics. *Nat Rev Neurosci* 8(10):743–754.
16. Mechoulam R, et al. (1995) Identification of an endogenous 2-monoglyceride, present in canine gut, that binds to cannabinoid receptors. *Biochem Pharmacol* 50(1):83–90.
17. Sugiura T, et al. (1995) 2-Arachidonoylglycerol: A possible endogenous cannabinoid receptor ligand in brain. *Biochem Biophys Res Commun* 215(1):89–97.
18. Stella N, Schweitzer P, Piomelli D (1997) A second endogenous cannabinoid that modulates long-term potentiation. *Nature* 388(6644):773–778.
19. Fu J, et al. (2003) Oleyethanolamide regulates feeding and body weight through activation of the nuclear receptor PPAR-alpha. *Nature* 425(6953):90–93.
20. Kathuria S, et al. (2003) Modulation of anxiety through blockade of anandamide hydrolysis. *Nat Med* 9(1):76–81.
21. Cravatt BF, et al. (2001) Supersensitivity to anandamide and enhanced endogenous cannabinoid signaling in mice lacking fatty acid amide hydrolase. *Proc Natl Acad Sci USA* 98(16):9371–9376.
22. Young LJ, Barrett CE (2015) Neuroscience. Can oxytocin treat autism? *Science* 347(6224):825–826.
23. Peñagarikano O, et al. (2015) Exogenous and evoked oxytocin restores social behavior in the *Cntnap2* mouse model of autism. *Sci Transl Med* 7:271ra8.
24. Kelley AE (2004) Ventral striatal control of appetitive motivation: Role in ingestive behavior and reward-related learning. *Neurosci Biobehav Rev* 27(8):765–776.
25. Trezza V, Baarendse PJJ, Vanderschuren LJMJ (2010) The pleasures of play: Pharmacological insights into social reward mechanisms. *Trends Pharmacol Sci* 31(10):463–469.
26. Cassano T, et al. (2011) Evaluation of the emotional phenotype and serotonergic neurotransmission of fatty acid amide hydrolase-deficient mice. *Psychopharmacology (Berl)* 214(2):465–476.
27. Haller J, Varga B, Ledent C, Barna I, Freund TF (2004) Context-dependent effects of CB<sub>1</sub> cannabinoid gene disruption on anxiety-like and social behaviour in mice. *Eur J Neurosci* 19(7):1906–1912.
28. Panksepp JB, Lahvis GP (2007) Social reward among juvenile mice. *Genes Brain Behav* 6(7):661–671.
29. Gerdeman GL, Lovinger DM (2003) Emerging roles for endocannabinoids in long-term synaptic plasticity. *Br J Pharmacol* 140(5):781–789.
30. Giuffrida A, et al. (1999) Dopamine activation of endogenous cannabinoid signaling in dorsal striatum. *Nat Neurosci* 2(4):358–363.
31. Mathur BN, Lovinger DM (2012) Endocannabinoid-dopamine interactions in striatal synaptic plasticity. *Front Pharmacol* 3:66.
32. Franklin K, Paxinos G (2004) *The Mouse Brain in Stereotaxic Coordinates* (Gulf Professional Publishing, Houston).
33. Astarita G, Piomelli D (2009) Lipidomic analysis of endocannabinoid metabolism in biological samples. *J Chromatogr B Analyt Technol Biomed Life Sci* 877(26):2755–2767.
34. Giuffrida A, Rodriguez de Fonseca F, Piomelli D (2000) Quantification of bioactive acylethanolamides in rat plasma by electrospray mass spectrometry. *Anal Biochem* 280(1):87–93.
35. Preibisch S, Saalfeld S, Tomancak P (2009) Globally optimal stitching of tiled 3D microscopic image acquisitions. *Bioinformatics* 25(11):1463–1465.
36. Silverman JL, Yang M, Lord C, Crawley JN (2010) Behavioural phenotyping assays for mouse models of autism. *Nat Rev Neurosci* 11(7):490–502.
37. Perello M, et al. (2010) Ghrelin increases the rewarding value of high-fat diet in an orexin-dependent manner. *Biol Psychiatry* 67(9):880–886.